Any immersion remote refocus (AIRR) microscopy

This project is maintained by amsikking in the York lab, and was funded by Calico Life Sciences LLC

Research article

Note that this is a limited PDF or print version; animated and interactive figures are disabled. For the full version of this article, please visit one of the following links: https://amsikking.github.io/any_immersion_remote_refocus_microscopy

Any immersion remote refocus (AIRR) microscopy

Alfred Millett-Sikking[1*]

[1]*Calico Life Sciences LLC, South San Francisco, CA 94080, USA*

[*] *Institutional email: amsikking+AIRR@calicolabs.com ; Permanent email: amsikking+AIRR@gmail.com*

Group website: andrewgyork.github.io

Abstract

3D imaging is essential for studying many biological processes. In microscopy it is traditional to take a series of 2D images at different depths by moving the objective lens or the sample. To avoid aberrations we match the refractive index (RI) of the sample to the immersion medium of the objective, an awkward constraint for microscope users and designers. Here, we present a versatile approach to aberration-free 3D imaging, where an objective of any immersion medium can be combined with a sample of any RI. For example, we can use a high numerical aperture (NA) air objective (Nikon 40x0.95) to look into a watery sample (RI ~ 1.33), and use remote refocus optics to extend the accessible depth from ~6μm to ~151μm. Avoiding liquid immersion is convenient for users and great for automated microscopy. Similarly, we can extend the depth of a high NA oil objective (Nikon 40x1.30) from ~8μm to ~65μm in water, and enjoy a larger field of view and NA compared to the

equivalent water immersion objective. We can apply this method to use different objectives on the same system, with maximum depth, immersion-free and maximum NA modalities. In addition, we present a dynamic zoom lens to enable fast RI tuning in the range 1.33-1.51, which maximizes performance for a diverse set of biological samples. By combining different objectives with dynamic remote refocus optics we can make an 'any immersion' microscope with a boosted focal range.

Intended audience

Microscope users, builders and developers.

Peer review status

First published _blank_ (This article is not yet peer-reviewed)

Cite as: _blank_

Introduction

Imaging samples in 3D is essential for studying many biological processes. In microscopy, we often collect 3D data by taking a series of 2D images at different depths in a sample. The image series can then be reconstructed in post processing to make a volume that we can explore. We can think of each 2D image as being a different 'focal plane' in the sample, where we use the 'focus' or a 'focusing' technique to change the depth.

Here we describe two different focus methods that we refer to as "standard focus" and "remote refocus" (RR), and discuss how they are typically restricted to a particular sample refractive index (RI). We then show a new way to use RR optics with any sample RI, and how to use RR with different objectives to make an "any immersion" microscope. In the simulations section, we model the standard focus depth and show how we can extend the depth with RR optics, including a dynamic RR design. In the data section, we demonstrate the power of the 'any immersion' concept by imaging deep into a watery sample with a high numerical aperture (NA) air objective that would normally give very blurry images. For the discussion section, we consider an attractive microscope design and review the main benefits of the technology.

We gear most of the article towards exploring new design options for high NA 3D microscopy. In particular, the configurations we explore here are readily applied to systems with existing RR optics, like single-objective light-sheet (SOLS) microscopes. However, we note that the methods are not limited to this regime, and compelling applications may be found with lower NA and larger field of view systems.

Theory

Here we present the essential concepts of standard focus and remote refocus (RR), and how they may be used together to make an any immersion microscope. We limit the theory to setups that use 'coverslip corrected'

microscope objectives, where the sample is separated from the objective by a coverslip and an immersion medium (Figure 1). We assume ideal imaging conditions throughout, with a correctly specified coverslip, a homogenous refractive index (RI) for the sample n_s and a homogenous RI for the immersion medium n_i.

Standard focus

To change the focal plane on a typical microscope we often move the objective towards and away from a stationary sample (Figure 2). Similarly, we can change the focal plane by moving the sample towards and away from a stationary objective. In either case we will refer to this method as "standard focus". For coverslip corrected microscope objectives, the depth of standard focus is mechanically limited by the distance between the front of the objective and the coverslip, usually called the working distance (WD) (Figure 1). However, the useful depth of standard focus may be dramatically reduced by the choice of sample RI, which is an awkward reality for microscope users and designers. To understand (and avoid) this effect we can consider the focusing process in more detail.

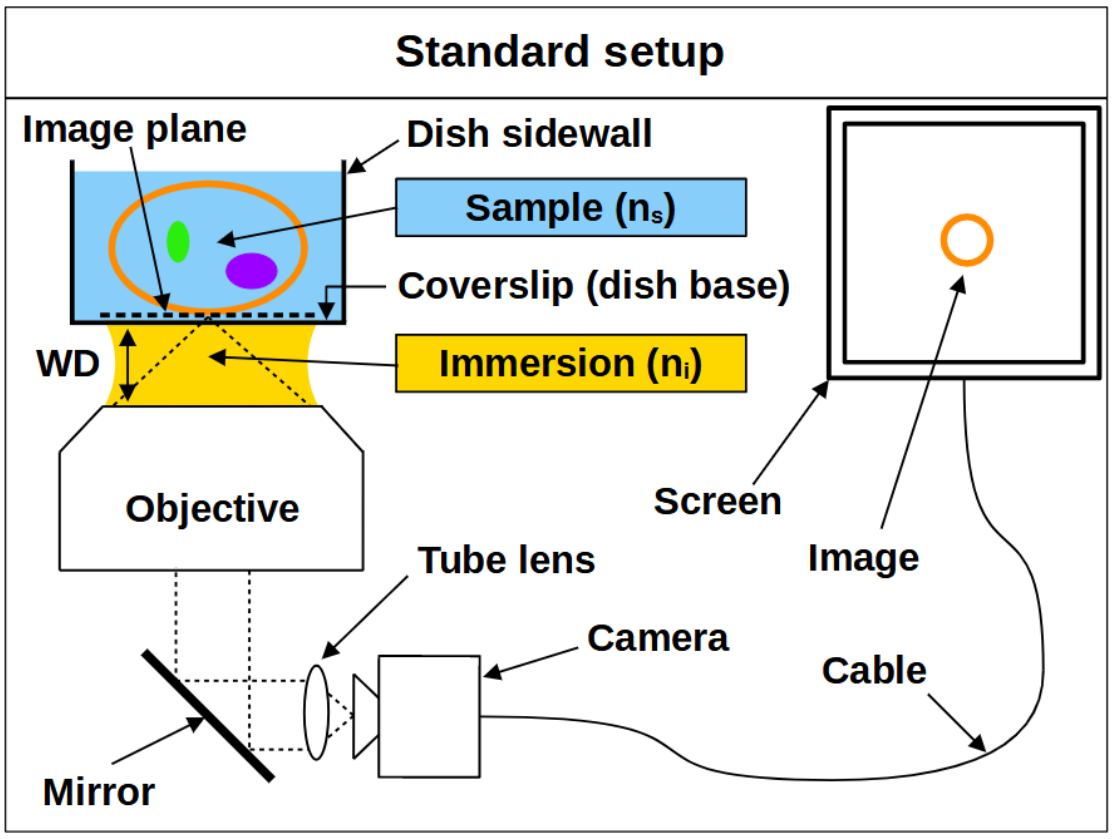

Figure 1: Setup showing a sample imaged by a coverslip corrected objective. This cartoon shows a watery 3D sample (like a cell in media) being imaged by a standard microscope (**objective + mirror + tube lens**). The **image** (which corresponds to the **image plane**) is formed at the **camera** and displayed on the cartoon **screen** (via the **cable**). The **sample** has a homogenous refractive index (RI) n_s, the **coverslip** is correctly specified (the base of the **dish**) and the **immersion** medium has a homogenous RI n_i. **WD** is the 'working distance' of the objective.

We can think of the space between the front of an objective and the image plane as containing the 'final elements' in the lens. For a coverslip corrected objective, this includes a coverslip of known specification (e.g. 170μm of glass) and an immersion medium of known type (e.g. air, water or oil). In particular the thickness and RI of the coverslip and immersion medium are important, and deviating from the intended values can produce severe aberrations, especially at high NA. A typical way to avoid aberrations is to place the sample directly onto the correct coverslip, and then image just above the coverslip using the correct immersion medium. This ensures the final elements of the objective are arranged as intended, but fixes the focal plane at 'depth zero' (i.e. just above the coverslip). So if we want to image deeper into the sample, we need some way of adjusting the focal plane without causing aberrations.

When we use standard focus to adjust the focal plane, for example by moving the objective towards the coverslip, we effectively push the image plane deeper into the sample (Figure 2). This motion reduces the thickness of the immersion medium, and increases the thickness of the sample that the objective must image through. Standard focus therefore changes the final elements in the lens, where layers or 'slabs' of intended immersion medium are effectively exchanged for slabs of sample. If the sample RI differs from the immersion medium, then the slab of sample will produce spherical aberration, and make the images blurry with increasing depth (Figure 2, 2/3 and 3/3) [Pawley 2006]. However, if we *match* the sample RI to the immersion medium RI then the objective is not disturbed by the slab of sample, so it will image as designed and standard focus will work as intended (Figure 2, 1/3).

So in summary, for standard focus we must match the sample refractive index to the immersion medium refractive index to avoid aberrations:

$$n_i = n_s \tag{1}$$

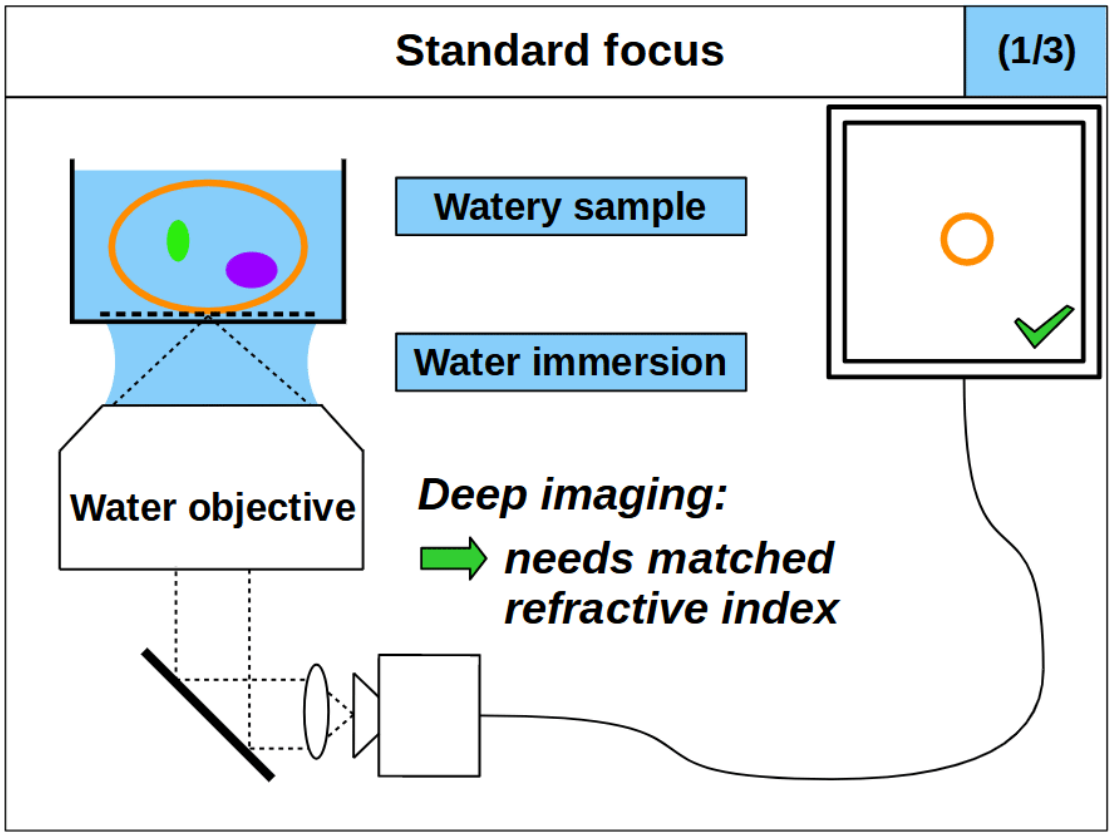

Figure 2: Standard focus into a watery sample with water, air and oil immersion. This cartoon shows a watery 3D sample (like a cell in media) being imaged at different depths by a standard microscope (objective + tube lens). The image is formed at the camera and displayed on the cartoon screen, which shows image planes at different depths in the sample as the objective moves up and down. **Animation 1/3** shows a water immersion objective that is refractive index (RI) *matched* to the sample, giving good images at depth. **Animation 2/3** shows an air objective that is RI *mismatched* to the sample and therefore gives blurry imaging from depth induced spherical aberration. **Animation 3/3** shows an oil immersion objective that (like animation 2/3) is also RI *mismatched* giving blurry images with depth.

For standard focus our need to match the sample RI to the immersion medium RI is awkward. The RI of biological samples varies significantly (range 1.33-1.51), leaving microscope users and designers chasing around between different immersion mediums, often with no correct solution. Air immersion (RI 1.0) is the most convenient and is excellent for high-speed tiling, but it has the lowest NA and low depth penetration due to the large RI difference. Water immersion (RI 1.33) is usually a good RI match for live samples, but it requires regular hydration (from evaporation) and has the lowest NA of the liquid immersions. Oil immersion (RI 1.51) offers the highest NA, and is insensitive to coverslip thickness, but struggles with depth from the RI mismatch. A good compromise between NA and RI matching is silicone oil immersion (RI 1.40), but this is still cumbersome in tiling applications, where the the oil must be continuously applied to maintain imaging.

Remote refocus

As an alternative to standard focus, remote refocus (RR) optics can also be used to image different focal planes in the sample. RR has become an important foundation in high-speed 3D imaging applications [Millett-Sikking 2018], most notably in the recent uptake of single-objective light-sheet (SOLS) microscopes [Millett-Sikking 2019, E. Sapoznik 2020, Chang 2021, Yang 2022, Chen 2022]. Here we summarize the main concepts of RR, and show how to extend their use beyond the traditional format. For a thorough treatment of RR theory we recommend the original paper [Botcherby 2007].

The main feature of RR optics is the ability to create an aberration-free 3D copy of the sample in a remote space, which we can then re-image with another microscope (Figure 3). We can then look at different focal planes without moving the primary objective or the sample, for example by moving one of the downstream objectives (Figure 4). This is quite different to a standard microscope (Figure 1), where the optics produce an aberration-free 2D image with substantial magnification (e.g. 100x). The magnification is of course by design so we can see small objects, but it has the side effect of distorting and aberrating the 3D copy. However, it is possible to create a 'perfect' 3D copy of the sample if we configure an optical system which produces uniform magnification in all directions [Maxwell 1858]. Specifically, we can get an aberration-free volume when we set the magnification M_{RR} between the sample and the remote space according to [Botcherby 2007]:

$$M_{RR} = \frac{n_1}{n_2} \tag{2}$$

where n_1 is the RI of the sample *and* the RI of immersion medium, and n_2 is the RI of the remote space.

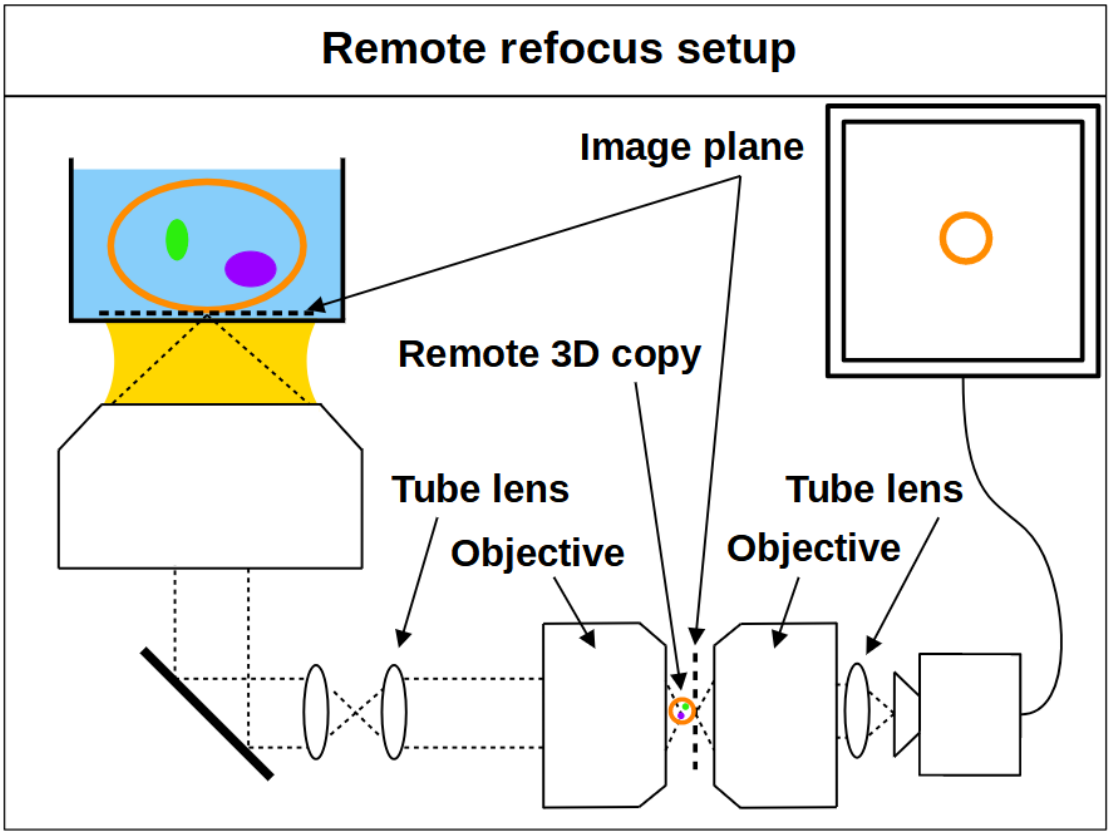

Figure 3: Setup showing a remote refocus microscope. This cartoon shows a watery 3D sample (like a cell in media) being imaged by a remote refocus (RR) microscope (a standard microscope + 2 additional microscopes). The optics in the first 2 microscopes (standard microscope + tube lens + objective) are configured to produce a **remote 3D copy** of the sample, which is then re-imaged by the 3rd microscope (objective + tube lens).

With RR optics it is traditional to *assume* that the sample RI matches the immersion medium RI (equation 1), and to set the RR magnification for the immersion medium:

$$M_{RR} = \frac{n_i}{n_2} \tag{3}$$

However, there are many situations where equations 1 and 3 do not apply, for example, when using an air objective with a watery sample, or when the sample RI differs from the RI of the typical immersion mediums. Here we explore the case where the sample RI and immersion medium RI are not matched:

$$n_i \neq n_s \tag{4}$$

We know from our review of standard focus that RI mismatch (equation 4) will reduce the depth of standard focus due to depth induced spherical aberration. However, we also know that we can adjust standard focus to get at least one aberration-free image plane, the image plane just above the coverslip, where any disturbance from the sample is minimal. In this special case, the RR can still produce an aberration-free volume if we set the magnification for the *sample*:

$$M_{RR} = \frac{n_s}{n_2} \tag{5}$$

This is a powerful concept. For example, we can build a microscope with RR optics configured for watery samples (equation 5, n_s = 1.33) and then use different types of immersion objective for this sample RI (Figure 4). For each objective we can use standard focus to find an aberration-free image plane, and then use the RR optics to access aberration-free 3D volumes, with different benefits in each configuration. For example, the water immersion objective has the **maximum depth** (Figure 4, 1/3), since standard focus still operates as intended. The air objective is **immersion-free** (Figure 4, 2/3) and the oil objective can have the **highest NA** (Figure 4, 3/3).

So in summary, we should set the remote refocus magnification for the refractive index of the sample, not the refractive index of the immersion medium.

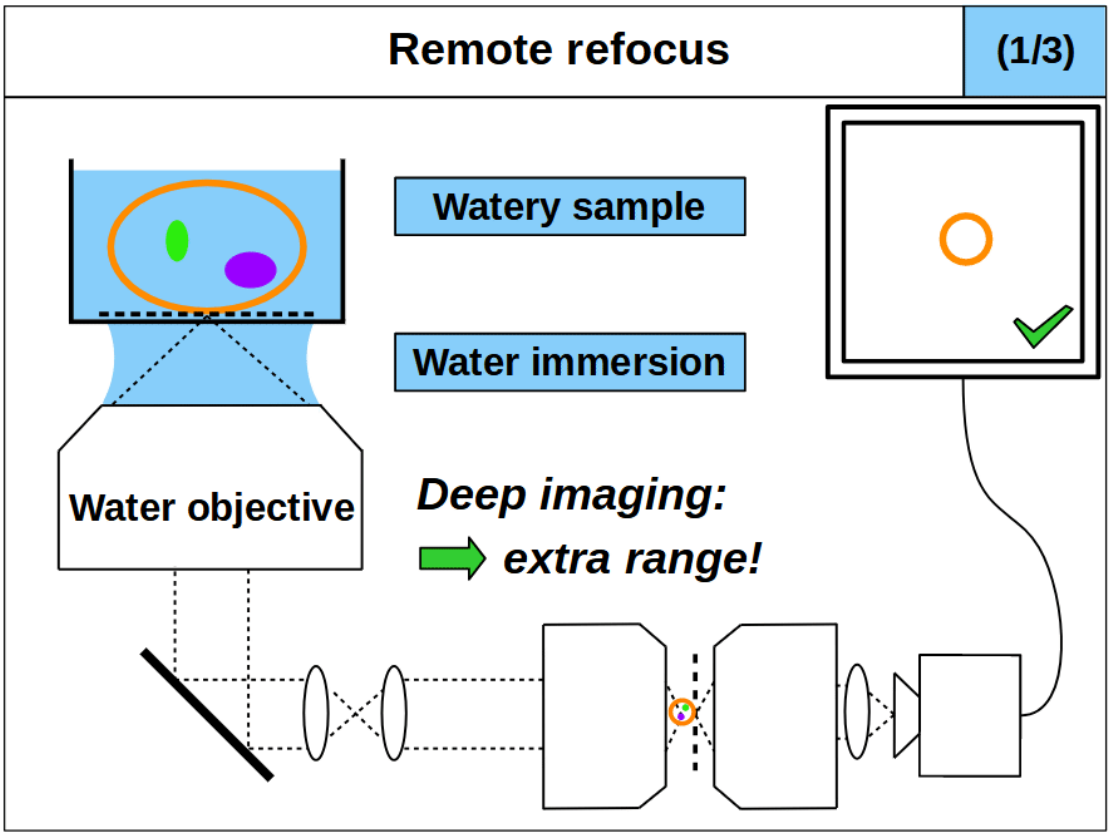

Figure 4: Remote refocus into a watery sample with water, air and oil immersion. This cartoon shows a watery 3D sample (like a cell in media) being imaged at different depths by a remote refocus (RR) microscope (a standard microscope + 2 additional microscopes). The optics in the first 2 microscopes (standard microscope + tube lens + objective) are configured to produce an aberration-free 3D copy of the sample in the remote space, which is then re-imaged by the 3rd microscope (objective + tube lens). **Note: the RR optics are set for a watery sample, regardless of the immersion used by the primary objective.** The final image is formed at the camera and displayed on the cartoon screen, which shows image planes at different depths in the sample as the objective in the 3rd microscope moves back and forth. **Animation 1/3** shows a water immersion objective that is refractive index (RI) *matched* to the sample. In this configuration the standard focus and RR both have **maximum depth**, although only the RR depth is animated here (giving extra depth over standard focus). **Animation 2/3** shows an air objective that is RI *mismatched* to the sample, greatly reducing the useful depth of standard focus. However, the RR is still optimized for a watery sample, and so the RR depth persists. Deeper **immersion-free** microscopy is available in this configuration. **Animation 3/3** shows an oil immersion objective that (like animation 2/3) is also RI *mismatched* (reducing the depth of standard focus). However, like animation 2/3, the RR is still optimized for a watery sample and so the RR depth persists. Deeper **maximum NA** microscopy is available in this configuration.

Any immersion remote refocus

In the previous sections we explored the mechanisms and limitations of standard focus and remote refocus (RR), and proposed a new way to use them together. In particular, we discussed how we can use standard focus to select an aberration-free image plane in a sample with any RI, and that we can do this using an immersion objective of any kind. We then discussed how we can use RR optics to access different focal planes

for any sample RI (equation 5). Here, we use these insights to consider new microscope design options, where we combine standard focus and RR optics to produce different modes of operation:

- **Maximum depth:** we can try to match the sample RI to the immersion medium RI and maximize the usable depth of standard focus (e.g. Figure 4, 1/3). Here the RR optics provide extra depth on top of standard focus, beyond the working distance of the objective. In the special case where we have a perfect RI match (equation 1), then this configuration reverts to the traditional mode of operation (equation 3).
- **Immersion-free:** we can combine a high NA air objective (with very limited standard focus depth in liquids) with RR optics optimized for liquid (e.g. Figure 4, 2/3). Avoiding liquid immersion is very convenient for users and great for automated microscopy, like time-lapse imaging or high-speed tiling.
- **Maximum NA:** we can combine a high NA oil objective (with very limited standard focus depth in watery samples) with RR optics optimized for water (e.g. Figure 4, 3/3). Oil immersion is coverslip insensitive and offers the maximum NA for live biological samples, exceeding that of high quality water immersion objectives.
- **Any sample RI:** by decoupling the choice of immersion medium from how we configure the RR optics, we can set the RR optics (via equation 5) to image deeper into any sample RI. For example, we can continuously tune the RR for any sample RI in the range 1.33-1.51 (Figure 7) and access aberration-free volumes that have traditionally been unavailable.

We can combine the above modes on the same instrument, with maximum depth, immersion-free and maximum NA modalities for any sample RI. **So, by combining different objectives with dynamic remote refocus optics we can make an 'any immersion' microscope with a boosted focal range.**

Simulations

To evaluate the deeper imaging potential of a remote refocus (RR) microscope (Figure 3) compared to a standard setup (Figure 1), we take a practical approach and model how a series of commercially available objectives compare in each configuration. For the sake of simplicity, we limit our search to a collection of Nikon objectives that are compatible with SOLS microscope design (a compelling use case for RR optics). We can therefore constrain the numerical aperture, focal length and immersion medium for a given setup, although we point out that these ideas can be applied to other manufacturers, and at lower NA. We can then calculate the standard focus and remote refocus depths as a function of the sample refractive index n_s over the biological range:

$$1.33 \leq n_s \leq 1.51 \tag{6}$$

Standard focus depth

In Figure 5 we compare the accessible imaging depth of different objectives in a standard microscope. In particular we plot the diffraction limited depth of standard focus as a function of the sample RI according to equation a8. The interactive figure can be toggled between linear and log scales for the highest NA objectives, and those with the 'most pixels' (N_{px}). For example, in the high NA category, the 100x1.35 silicone oil objective

offers the best compromise for varying sample types, with a minimum depth of 10μm for any sample RI. However, if the samples are mostly aqueous, then the 60x1.27 water lens has a much larger depth (limited by the working distance at 180μm). The 40x0.95 air objective is perhaps the worst option for depth, offering only ~6μm for any liquid sample (visible on the log scale). The 100x1.45 oil may be the least attractive option for live biology, with the inconvenience of liquid immersion and the lowest depth in watery samples (forcing the 3μm lower bound). Similar trends can be seen in the most pixels category.

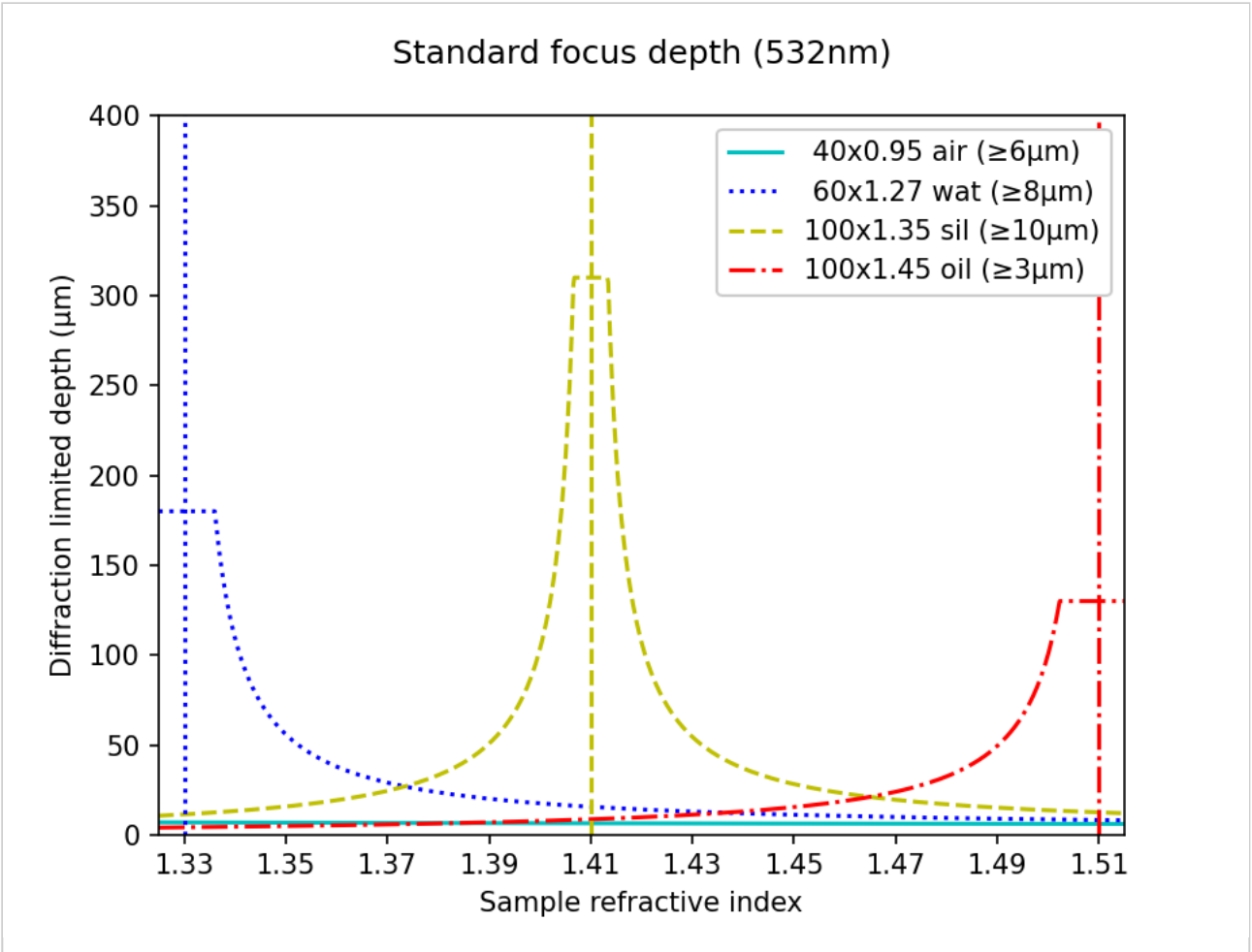

Nikon objectives: Highest NA Depth scale: linear

Figure 5: the standard focus depth of a microscope. The diffraction limited imaging depth is plotted as a function of sample refractive index for a collection of Nikon objectives at 532nm (equation a8). The figure is interactive and can be toggled between linear and log scales for objectives with the highest NA and those with the most pixels. The curves are truncated at the working distance of each objective and vertical reference lines are added for the standard immersion types (water=1.33, silicone=1.41 and oil=1.51).

Standard focus and remote refocus depth

In Figure 6 we present the combined depth of a standard focus with RR optics according to equation a11. In this setup, the primary objectives are still limited to a particular immersion medium, but we can (in principle) tune the RR optics continuously across the range of the sample RI (shown here). All of the configurations now benefit from the extra depth provided by the RR optics. In particular, in the high NA category the lower bound on the 100x1.45 oil lens has now jumped from 3μm to 35μm, converting it into an attractive option for many

applications. In practice, this delivers deeper imaging at **maximum NA** for any sample RI under 1.45. Most apparent in the high NA category is the large increase in depth now available to the 40x0.95 air objective, offering **immersion-free** imaging up to 151µm!

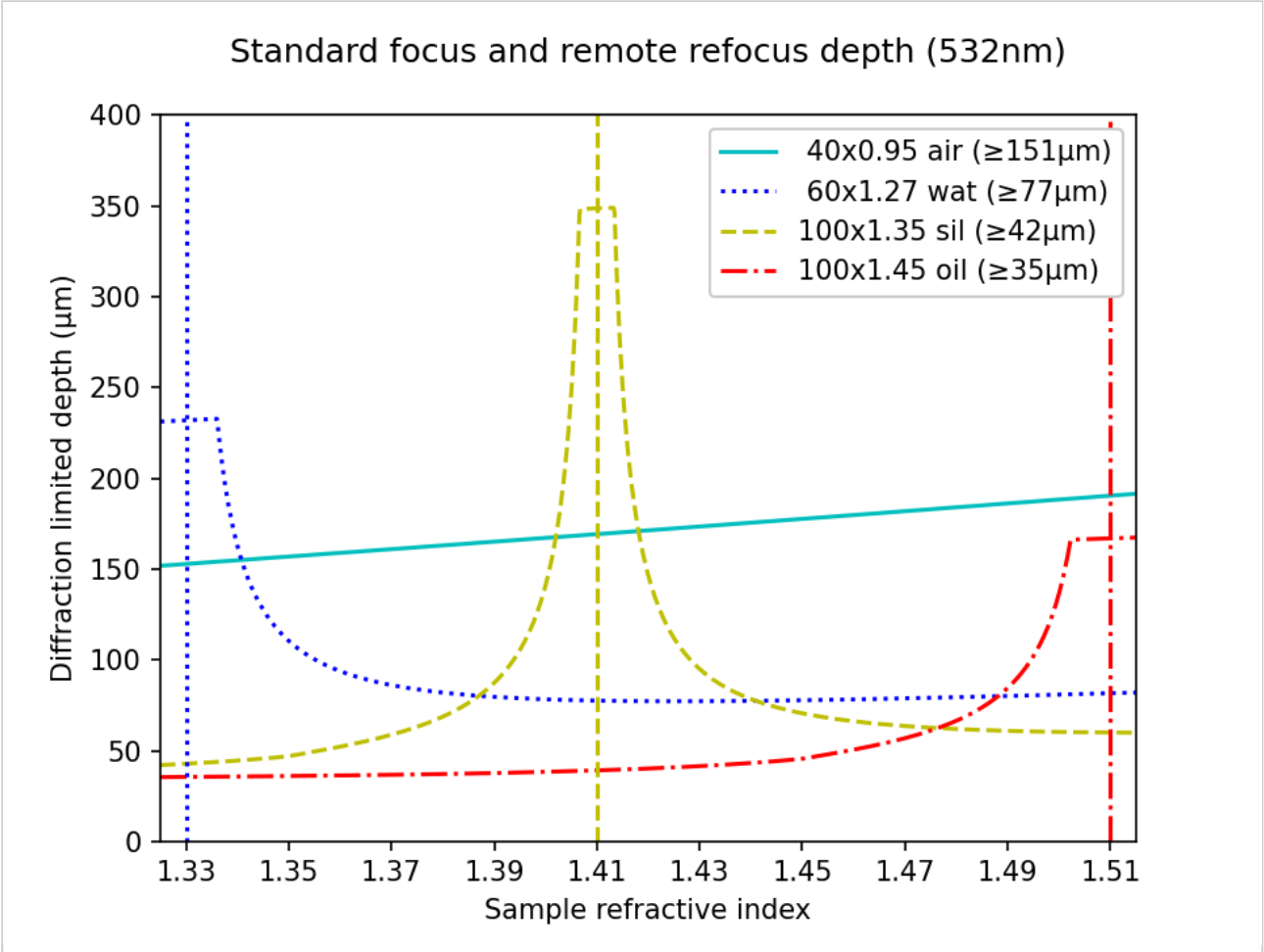

Nikon objectives: Highest NA ▾ Depth scale: linear ▾

Figure 6: the combined depth of a standard focus with remote refocus optics. The diffraction limited imaging depth is plotted as a function of sample refractive index for a collection of Nikon objectives at 532nm (equation a11). The figure is interactive and can be toggled between linear and log scales for objectives with the highest NA and those with the most pixels. The curves are truncated at the working distance of each objective and vertical reference lines are added for the standard immersion types (water=1.33, silicone=1.41 and oil=1.51).

Dynamic remote refocus

In the theory section for RR, we discuss how the magnification should be set for the sample RI, and not the immersion medium (equation 5). Previously, we used static optical configurations to set the RR magnification for the immersion medium RI (equation 3), with the hope that the sample RI would match [Millett-Sikking 2018, Millett-Sikking 2019].

Here we present a dynamic zoom lens to enable fast RR magnification tuning for the RI range 1.33-1.51. This allows us to continuously apply equation 5, and maximize RR performance for a diverse set of biological samples (Figure 7). Our design uses inexpensive stock parts, maintains constant track length and telecentricity,

and is diffraction limited across the visible spectrum and standard sCMOS field of view (see appendix for details). Specifically this module is intended to replace the tube lens in the second microscope of an RR system, and provides a concrete design to enable the focal depths shown in Figure 6.

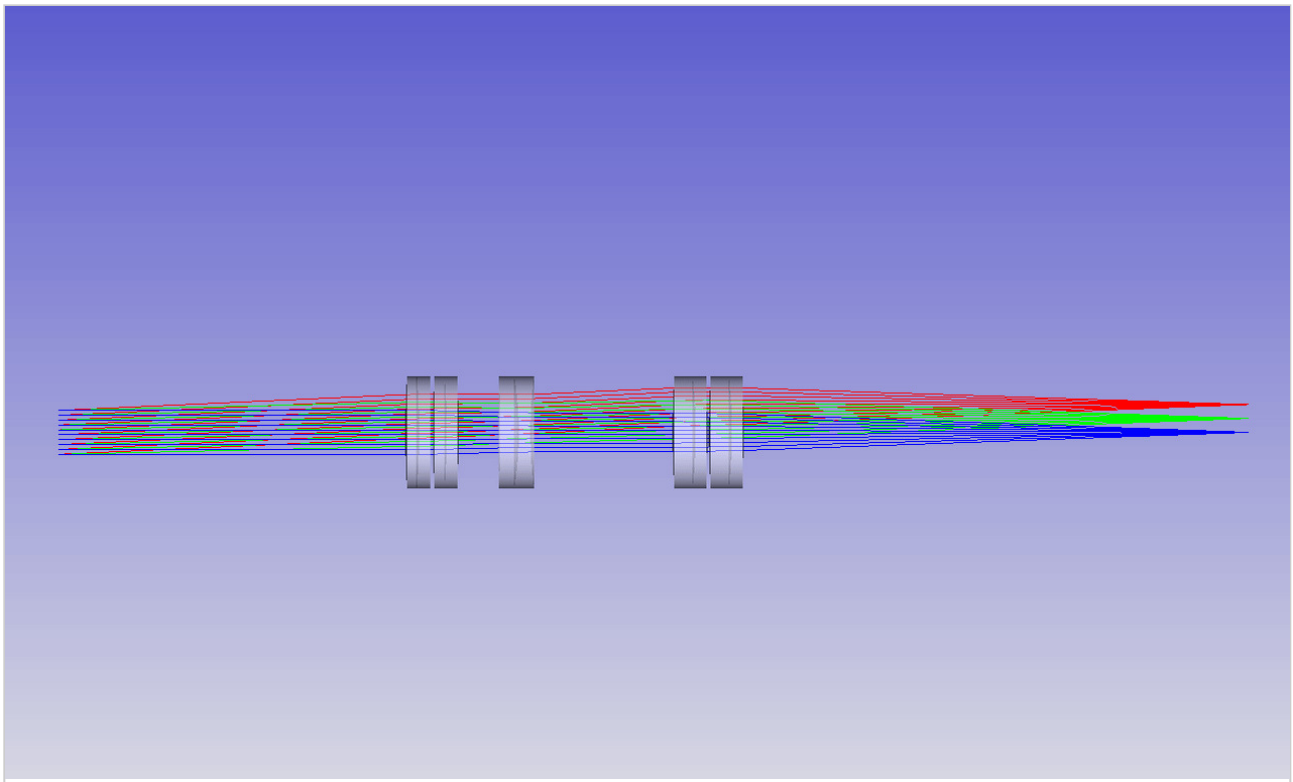

Figure 7: Dynamic zoom tube lens. This animation shows an example of a zoom lens that can replace a static tube lens in a remote refocus microscope. In this version the focal length varies continuously as the elements are moved, allowing the magnification of the RR to be tuned across the biological refractive index range 1.33-1.51. The lens uses inexpensive stock parts, maintains constant track length and telecentricity, and is diffraction limited across the visible spectrum and standard sCMOS field of view (see appendix for details).

Data

To demonstrate the power of the 'any immersion' concept we built a prototype large field of view SOLS microscope with (static) RR optics tuned for water (see here for instrument details). We then used this platform to directly **compare a Nikon 40x1.15 water objective against a Nikon 40x0.95 air objective imaging deep into a watery sample** (fluorescent beads in agarose). We picked this example since the RI mismatch between air and water is very high, which greatly reduces the usable depth of standard focus. However, the RR is unaffected by the RI mismatch, and the RR depth is substantial in this configuration, which really highlights the benefit of this new regime.

Water objective

We use the 40x1.15 water objective as the 'benchmark' for a typical optical configuration, where the immersion medium and sample have the same RI. In this mode the volumetric point spread function (PSF) is insensitive to

standard focus, so we can move the primary objective up and down to access different depths (Figure 8). The main benefits of this setup compared to the air objective are an increased NA and total focus depth (standard focus + RR), in exchange for the inconvenience of the water immersion.

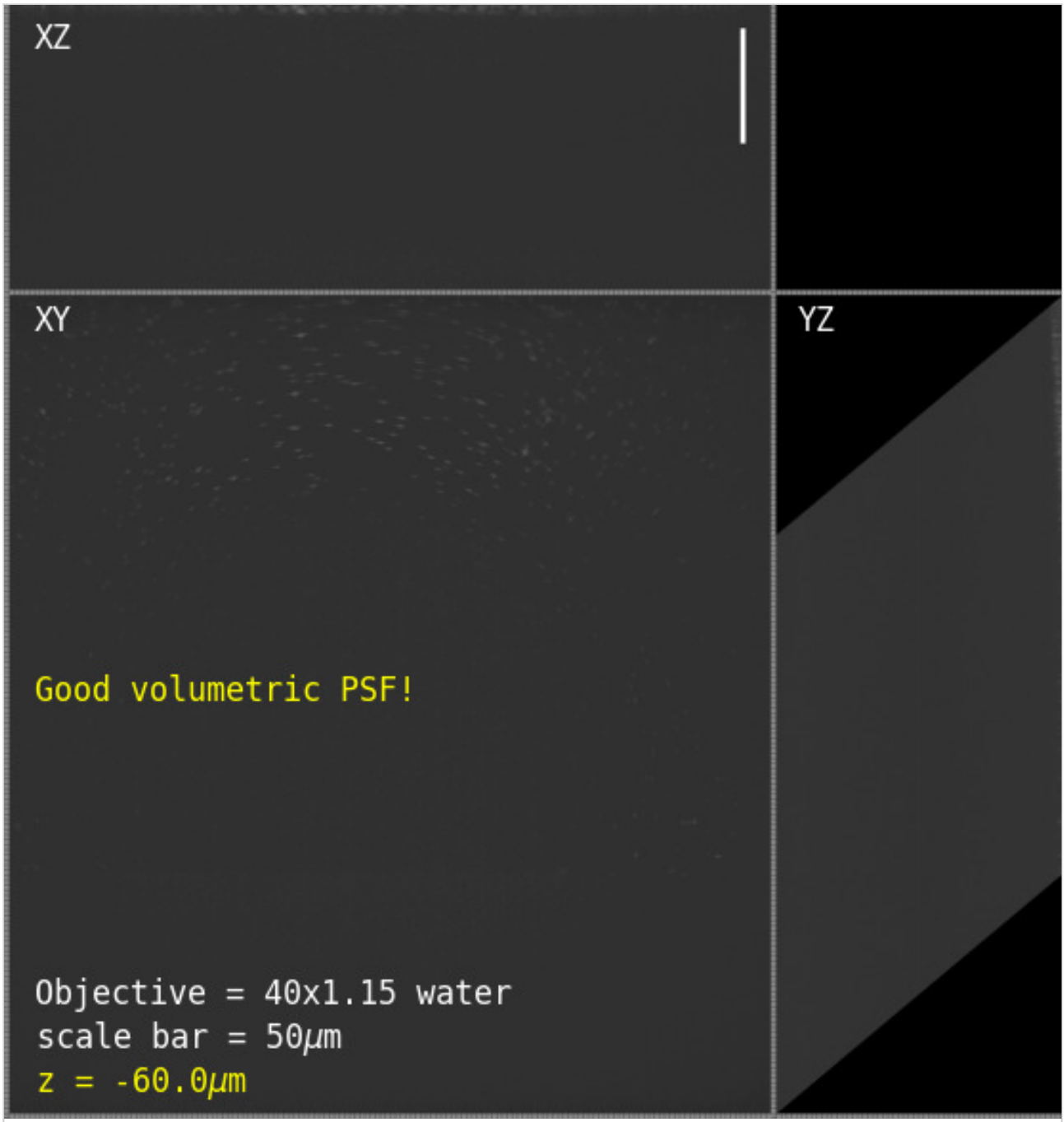

Figure 8: PSF vs standard focus for a 40x1.15 water objective. This animation shows the volumetric point spread function of a Nikon 40x1.15 water immersion objective as a function of standard focus (z). The fluorescent beads were prepared in a watery gel according to this protocol. Since the sample RI *matches* the water immersion the PSF is insensitive to standard focus, allowing an increased depth of focus (standard focus + RR) when using the microscope in this modality. **Note:** each frame of the animation shows the max projections of the entire volume (~330x355x125)μm^3 in traditional XY, XZ and YZ coordinates.

Air objective

We can now *swap* the 40x1.15 water objective for the 40x0.95 air objective on the same microscope and get good volumetric PSF deep into the watery gel! Because the objectives have the same effective focal length they conserve the RR magnification (equation 5). Normally the depth of standard focus is limited to about ~6μm (Figure 5), but here we can clearly image > 50μm with the RR optics (Figure 9). Compared to the water objective, this mode has the benefit of being immersion-free, with the drawback of slightly lower NA and a greatly reduced standard focus depth.

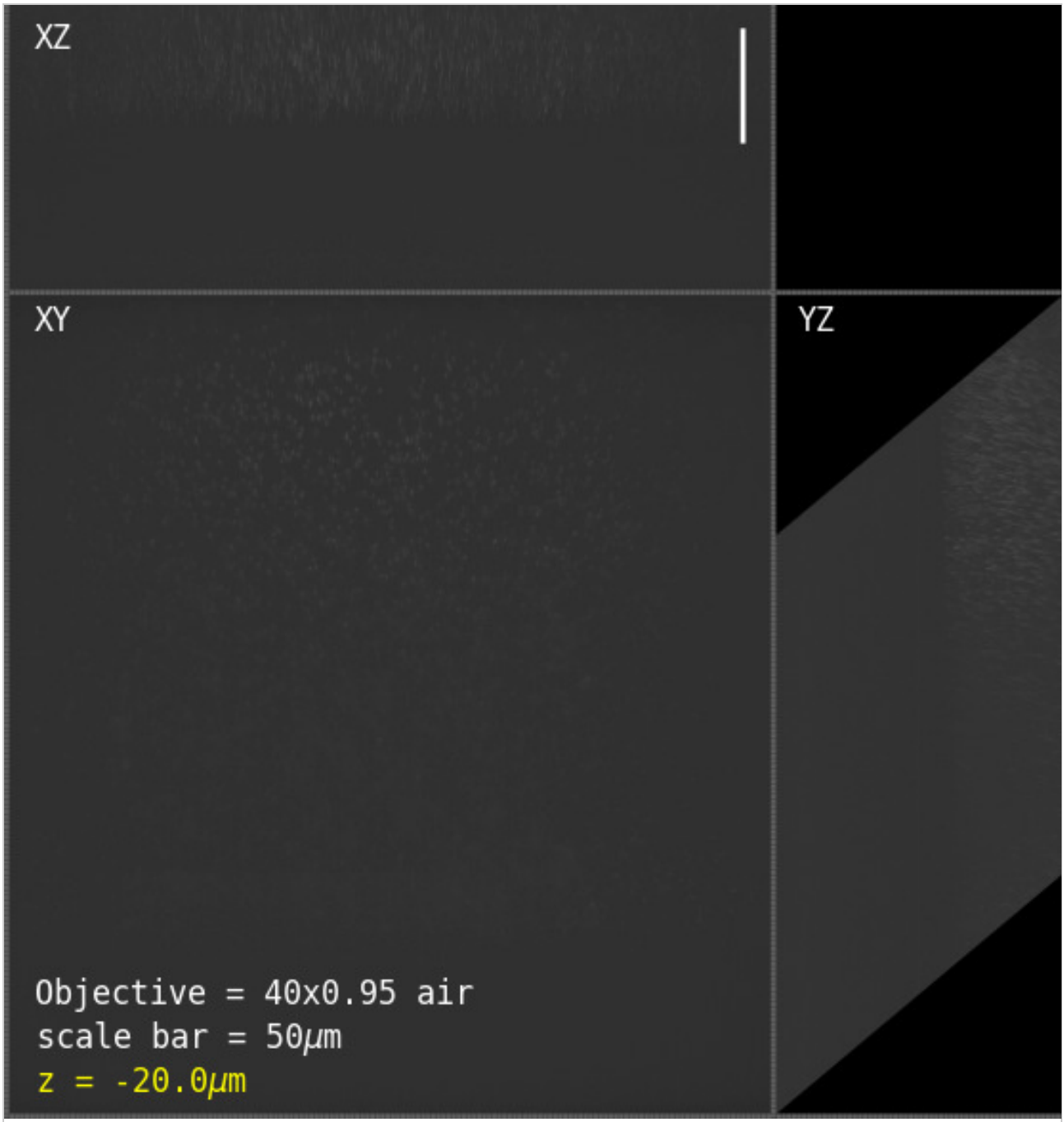

Figure 9: PSF vs standard focus for a 40x0.95 air objective. This animation shows the volumetric point spread function of a Nikon 40x0.95 air objective as a function of standard focus. The fluorescent beads were prepared in a watery gel according to this protocol. Since the sample RI strongly *mismatches* the air immersion the PSF is highly sensitive to standard focus. However, as predicted by the simulations, there is a ~6μm range over which the remote refocus volume is good, allowing deeper immersion-free imaging when using the microscope in this modality (i.e. for convenience or high speed tiling etc). **Note:** each frame of the

animation shows the max projections of the entire volume (~330x355x125)μm^3 in traditional XY, XZ and YZ coordinates.

Point spread function

If we 'park' the standard focus in a good place for both the water and air objectives (i.e. at 'zero' depth where the focal plane is just above the coverslip) then we can compare the PSF in both configurations over the volume (~330x195x65μm^3). For the **water objective PSF** we found full width half max (FWHM) values in the range **(425-582)nm laterally and (1.38±0.11)µm axially** (2577 beads used for statistics). For the **air objective PSF** we found FWHM values in the range **(422-550)nm laterally and (2.08±0.07)µm axially** (2716 beads).

As expected the water objective has notably improved axial PSF due to the higher NA. The higher NA should also show in a reduced radial PSF but the current instrument prototype was originally optimized for the air objective so there is some vignetting at objective 2 and the pixel size (~220nm) is too large (addressed here with an improved design). Overall these PSF results are in line with similar microscopes like DaXi which gave (380-480)nm lateral and (1.86±0.17)µm axial [Yang 2022] or tiling OPM with (390-430)nm lateral and (1.22±0.13)µm axial [Chen 2022].

Discussion

In contrast to a standard microscope (e.g. Figure 1), we have shown that we can use an RR microscope (e.g. Figure 3) to collect deeper aberration-free volumes for any combination of immersion medium and sample RI (Figure 6). The method is quite general, and applies to high and low NA systems with many configuration options. To highlight some of the advantages of this new design space, we target the discussion towards high NA systems for watery samples (RI ~1.33) that are most relevant to 3D time-lapse imaging (like living cells and organisms).

If we consider a standard microscope with a sample RI under ~1.37, then we can see from Figure 5 that the 60x1.27 water immersion objective has the highest diffraction limited depth in the high NA category. In this regime, the other objectives (air, silicone and oil immersion) are best used for shallow 3D samples (< 10µm) or speciality situations where the lack of liquid immersion or marginal increase in NA are required (like high-speed 2D tiling or TIRF microscopy). With a ~333µm field of view, a theoretical resolving power of ~250nm, and ~2600 pixels, the 60x water objective is a good match for current sCMOS cameras (specifications from table). However, water immersion objectives are sensitive to coverslip tilt and thickness, and require regular hydration.

If we now consider a microscope with RR optics set (via equation 5) for watery samples (RI ~ 1.33), we can see from Figure 6 that all of the objectives now have a boosted focal depth. For example, the depth of the 40x0.95 air objective has increased from ~6µm to ~151µm, offering an impressive volume with **immersion-free** speed and convenience. Also, the depth of the 40x1.30 oil objective has increased from ~8µm to ~65µm, offering an impressive volume with **maximum NA**. We can readily add a water immersion objective to the collection for **maximum depth**, for example the Nikon 40x1.15 water objective has a working distance of ~600µm (MRD77410). Because these objectives have the same focal length, they maintain the correct remote refocus

magnification (equation 5), and so they are *interchangeable* on the same system. In addition, at 40x magnification these objectives offer larger fields of view (~500μm) and pixel counts (> ~2927) than the 60x1.27 water (the leading option for a standard microscope).

We conclude that RR optics should be configured for the sample RI, and not the immersion medium of the objective (equation 5). We acknowledge that for the same or similar samples this may be achieved with static optical configurations. However, we present a dynamic zoom lens to quickly tune the RR optics for the refractive index range 1.33-1.51, which maximizes performance for a diverse set of biological samples. This has the additional benefit of avoiding the axial 'stretching' ($n_i > n_s$) and 'squashing' ($n_i < n_s$) distortions from focusing with mismatched RI [Diel 2020]. **We propose that a dynamic magnification compensator is the preferred way to build a remote refocus microscope when imaging samples of varied refractive index.**

We find the **immersion-free** regime particularly attractive for high throughput screening applications [Maioli 2016], where the benefit of high-speed tiling can greatly outweigh the slightly lower NA of an of air objective compared to liquid immersion options. In this mode, the increase in depth of a RR microscope over a standard microscope is substantial, for example ~325μm vs ~17μm for the 20x0.80 air objective (from the 'most pixels' category). We also find the thermal isolation from the 'air gap' appealing, avoiding the need to heat the objective for incubated samples. In addition, the stronger reflections from the air to coverslip boundary could be beneficial for hardware autofocus systems.

We see the coverslip insensitive oil immersion options with **maximum NA** as a great option for 3D super resolution [Zanacchi 2011] and low light experiments [Betzig 2006] that benefit from the highest angular collection at the primary objective. For example, the 40x1.30 oil objective from the 'most pixels' category has a large field of view (~500μm), and can now be considered near maximum NA for water samples up to ~65μm deep, making it an impressive option for many applications. We note that in the 'maximum NA' regime, the half angle of the remote objective may limit the collection half angle of the emission (e.g. ~72deg for a 0.95 air objective). However, the additional angular range at the primary objective can still be utilized for delivering excitation or autofocus light.

Given the 'mix and match' nature of the design space and the strong dependency on sample RI, we encourage builders to absorb the ideas presented here, run their own calculations, and then build the best system for their application.

Acknowledgements

This work was funded and supported by Calico Life Sciences LLC, and we would like to acknowledge the fantastic research environment that has been created here by the senior staff. We have enjoyed a spectacular level of freedom and support that has made this work possible.

In particular I acknowledge Andrew G. York for the innovative environment he has established at Calico, and his ongoing scientific mentorship and support.

Appendix

Additional details can be found in the appendix.

References

1. [Pawley 2006] Handbook of Biological Confocal Microscopy, third edition; J. Pawley; Springer US, ISBN 978-0-387-25921-5, eBook ISBN 978-0-387-45524-2, (2006) https://doi.org/10.1007/978-0-387-45524-2
2. [Millett-Sikking 2018] Remote refocus enables class-leading spatiotemporal resolution in 4D optical microscopy; A. Millett-Sikking, N.H. Thayer, A. Bohnert and A.G. York; (2018) https://doi.org/10.5281/zenodo.1146083
3. [Millett-Sikking 2019] High NA single-objective light-sheet; A. Millett-Sikking, K.M. Dean, R. Fiolka, A. Fardad, L. Whitehead and A.G. York; (2019) https://doi.org/10.5281/zenodo.3244420
4. [E. Sapoznik 2020] A versatile oblique plane microscope for large-scale and high-resolution imaging of subcellular dynamics; E. Sapoznik, B. Chang, J. Huh, R.J. Ju, E.V. Azarova, T. Pohlkamp, E.S. Welf, D. Broadbent, A.F. Carisey, S.J. Stehbens, K. Lee, A. Marín, A.B. Hanker, J.C. Schmidt, C.L. Arteaga, B. Yang, Y. Kobayashi, P.R. Tata, R. Kruithoff, K. Doubrovinski, D.P. Shepherd, A. Millett-Sikking, A.G. York, K.M. Dean and R.P. Fiolka; (2020) https://doi.org/10.7554/eLife.57681
5. [Chang 2021] Real-time multi-angle projection imaging of biological dynamics; B. Chang, J.D. Manton, E. Sapoznik, T. Pohlkamp, T.S. Terrones, E.S. Welf, V.S. Murali, P. Roudot, K. Hake, L. Whitehead, A.G. York, K.M. Dean and R.P. Fiolka; (2021) https://doi.org/10.1038/s41592-021-01175-7
6. [Yang 2022] DaXi—high-resolution, large imaging volume and multi-view single-objective light-sheet microscopy; B. Yang, M. Lange, A. Millett-Sikking, X. Zhao, J. Bragantini, S. VijayKumar, M. Kamb, R. Gómez-Sjöberg, A.C. Solak, W. Wang, H. Kobayashi, M.N. McCarroll, L.W. Whitehead, R.P. Fiolka, T.B. Kornberg, A.G. York and L.A. Royer; (2022) https://doi.org/10.1038/s41592-022-01417-2
7. [Chen 2022] Increasing the Field-of-View in Oblique Plane Microscopy via optical tiling; B. Chen, B. Chang, F. Zhou, S. Daetwyler, E. Sapoznik, G.M. Gihana, L.P. Castro, M.C. Sorrell, K.M. Dean, A. Millett-Sikking, A.G. York and R.P. Fiolka; (2022) https://doi.org/10.1364/BOE.467969
8. [Botcherby 2007] An optical technique for remote focusing in microscopy; E.J. Botcherby, R. Juškaitis, M.J. Booth and T. Wilson; Optics Communications, vol 281(4), p880-887, (2007) https://doi.org/10.1016/j.optcom.2007.10.007
9. [Maxwell 1858] On the general laws of optical instruments; J.C. Maxwell; Quart. J. Pure Appl. Maths., vol 2, p233, (1858) https://ia800908.us.archive.org/24/items/scientificpapers01maxw/scientificpapers01maxw.pdf
10. [Diel 2020] Tutorial: avoiding and correcting sample-induced spherical aberration artifacts in 3D fluorescence microscopy; E.E. Diel, J.W. Lichtman and D.S. Richardson; (2020) https://doi.org/10.1038/s41596-020-0360-2
11. [Maioli 2016] Time-lapse 3-D measurements of a glucose biosensor in multicellular spheroids by light sheet fluorescence microscopy in commercial 96-well plates; V. Maioli, G. Chennell, H. Sparks, T. Lana, S. Kumar, D. Carling, A. Sardini and C. Dunsby; (2016) https://doi.org/10.1038/srep37777
12. [Zanacchi 2011] Live-cell 3D super-resolution imaging in thick biological samples; F.C. Zanacchi, Z. Lavagnino, M.P. Donnorso, A.D. Bue, L. Furia, M. Faretta and A. Diaspro; (2011)

https://doi.org/10.1038/nmeth.1744

13. [Betzig 2006] Imaging Intracellular Fluorescent Proteins at Nanometer Resolution; E. Betzig, G.H. Patterson, R. Sougrat, O.W. Lindwasser, S. Olenych, J.S. Bonifacino, M.W. Davidson, J. Lippincott-Schartz and H.F. Hess; (2006) https://doi.org/10.1126/science.1127344